
INTEGRAL PROBABILITY METRIC BASED REGULARIZATION FOR OPTIMAL TRANSPORT

A PREPRINT

Piyushi Manupriya
Department of Computer Science
Indian Institute Of Technology Hyderabad
Kandi, Telangana. INDIA
CS18M20P100002@iith.ac.in

SakethaNath Jagarlapudi
Department of Computer Science
Indian Institute Of Technology Hyderabad
Kandi, Telangana. INDIA
saketha@cse.iith.ac.in

Pratik Jawanpuria
Microsoft IDC, INDIA
pratik.jawanpuria@microsoft.com

June 8, 2021

ABSTRACT

Regularization in Optimal Transport (OT) problems has been shown to critically affect the associated computational and sample complexities. It also has been observed that regularization effectively helps in handling noisy marginals as well as marginals with unequal masses. However, existing works on OT restrict themselves to ϕ -divergences based regularization. In this work, we propose and analyze Integral Probability Metric (IPM) based regularization in OT problems. While it is expected that the well-established advantages of IPMs are inherited by the IPM-regularized OT variants, we interestingly observe that some useful aspects of ϕ -regularization are preserved. For example, we show that the OT formulation, where the marginal constraints are relaxed using IPM-regularization, also lifts the ground metric to that over (perhaps un-normalized) measures. Infact, the lifted metric turns out to be another IPM whose generating set is the intersection of that of the IPM employed for regularization and the set of 1-Lipschitz functions under the ground metric. Also, in the special case where the regularization is squared maximum mean discrepancy based, the proposed OT variant, as well as the corresponding Barycenter formulation, turn out to be those of minimizing a convex quadratic subject to non-negativity/simplex constraints and hence can be solved efficiently. Simulations confirm that the optimal transport plans/maps obtained with IPM-regularization are intrinsically different from those obtained with ϕ -regularization. Empirical results illustrate the efficacy of the proposed IPM-regularized OT formulation.

This draft contains the main paper and the Appendices.

1 Introduction

Recently optimal transport (OT) has witnessed a lot of success in machine learning applications. Peyré and Cuturi [2019] is an excellent manuscript on this subject. OT's success is partly due to clever regularization, which seems to play a critical role in handling noisy marginals [Frogner et al., 2015], marginals of unequal masses [Chizat, 2017, Liero et al., 2018], in determining the computational complexity [Cuturi, 2013, Seguy et al., 2018], and the sample complexity [Mena and Niles-Weed, 2019, Genevay et al., 2019, Feydy et al., 2018, Nath and Jawanpuria, 2020].

Though regularization for OT is well-studied, surprisingly only ϕ -divergence based regularizers are popularly employed. As discussed in Sriperumbudur et al. [2009], Integral Probability Metrics (IPMs) are a complementary family of metrics over measures that exhibit intrinsically different properties. Also, in general, estimators for IPMs have better rates of convergence than those for ϕ -divergences [Sriperumbudur et al., 2009]. This is particularly helpful in high-dimensional settings. While it is expected that such well-established advantages of IPMs will be inherited by IPM-regularized

OT variants (for example see Theorem 2 in Nath and Jawanpuria [2020]), it is not clear if other useful aspects of ϕ -divergence based regularization are preserved.

This work takes the novel approach of employing IPM-based regularizers for OT. In particular, we study the OT variant where the marginal constraints are relaxed via appropriate IPM-regularization. We consider a generic setting where the marginal measures need not be normalized and may have different masses (for example, the unbalanced optimal transport set-up).

Interestingly, we show that some useful aspects of ϕ -divergence based regularization are indeed preserved with IPM-based regularizers. For example, it is well-known that divergence based OT formulations lift ground metrics to those over measures: Gaussian-Hellinger type metrics [Liero et al., 2018], etc. Like-wise, we show that the proposed IPM-regularized OT formulation also lifts the ground metric to that over (perhaps un-normalized) measures. Using a Kantorovich-type duality derivation, we show that the lifted metric turns out to be another IPM whose generating set is the intersection of that of the IPM employed for regularization and the set of 1-Lipschitz functions under the ground metric. This connection not only provides the right ‘‘Wasserstein-type’’ metric corresponding to the Kantorovich metric in the unbalanced setting, but also motivates us to define novel and useful loss functions based on powers of IPM-regularizers.

For example, when the regularizer is squared Maximum Mean Discrepancy (MMD), the proposed OT formulation, as well as the corresponding barycenter formulation, turn out to be those of minimizing a convex quadratic subject to non-negativity constraints and hence can be solved efficiently using algorithms like projected gradient descent, mirror descent, etc. This helps in scaling to moderately large ML applications. We present a couple of applications, where simulations show instances where the squared-MMD regularized OT outperforms popular KL-divergence regularized OT.

Finally, the form/shape/characteristics of the optimal transport plan critically depend on the regularization: for instance, the Sinkhorn transport plan is always Gaussian [Janati et al., 2020] with Gaussian marginals. We empirically observe that this is not the case with the MMD-based regularizers. Unlike the ϕ -divergence regularizers, the support of the transport plan marginals can be different from those of source/target marginals with the proposed IPM-regularizers. This might be useful in cases where support constraints for the transport plan exist [Korman and McCann, 2012]. Thus, our framework offers immense flexibility for employment in diverse applications.

We end this section with a summary of the main contributions:

- IPM-regularization for OT is not well-studied. We make a novel attempt to study this and contrast it with the popular ϕ -divergence based regularization.
- We show that IPM-regularization in the (unbalanced) OT setting lifts the ground metric to that between (arbitrary) measures. We prove that these lifted metrics are again IPMs (with specific generating sets).
- We propose a new family of loss functions based on powers of IPM-regularizers and demonstrate that they have immense potential in ML applications.
- We present simulation results on a couple of ML applications, where we show instances where the proposed IPM-regularization outperforms KL-divergence based regularization. In addition, we empirically contrast the characteristics of the transport plan obtained by the two regularization schemes.

Proof of all the theoretical results are provided in the supplementary material. The rest of the paper is organized as follows. Section 2 provides a summary of the IPM and OT literature. In Section 3, we discuss the proposed problem formulation, its properties, and efficient algorithms for its solution. Section 4 discusses the empirical results. In Section 5, we discuss the connection of the proposed IPM regularizers with robustness and the flexibility they enjoy with respect to support constraints. Section 6 concludes the paper.

2 Preliminaries

In this section we summarize necessary basic results from IPM and OT literature. We begin with some notations.

Let \mathcal{X} be a set (domain) that forms a compact Hausdorff space. Let $\mathcal{R}(\mathcal{X})$ denote the set of all non-negative (finite) Radon measures defined over \mathcal{X} ; while the set of all probability measures is denoted by $\mathcal{R}_1(\mathcal{X})$. For a measure on the product space, $\pi \in \mathcal{R}(\mathcal{X} \times \mathcal{X})$, let π_1, π_2 denote the first and second marginals respectively (i.e., they are the push-forwards under the canonical projection maps onto \mathcal{X}). Let $\mathcal{L}(\mathcal{X})$ denote the set of all real-valued measurable functions over \mathcal{X} .

2.1 Integral Probability Metrics

Given a set $\mathcal{G} \subset \mathcal{L}(\mathcal{X})$, the Integral Probability Metric (IPM) [Muller, 1997, Sriperumbudur et al., 2009, Agrawal and Horel, 2020] associated with \mathcal{G} , is defined by:

$$\gamma_{\mathcal{G}}(\mu, \nu) \equiv \max_{f \in \mathcal{G}} \left| \int_{\mathcal{X}} f \, d\mu - \int_{\mathcal{X}} f \, d\nu \right| \quad \forall \mu, \nu \in \mathcal{R}(\mathcal{X}). \quad (1)$$

Classical examples of IPMs include:

Kantorovich: Let d be a given (ground) metric over the domain \mathcal{X} . Let, $\|f\|_d \equiv \max_{x \in \mathcal{X} \neq y \in \mathcal{X}} \frac{|f(x) - f(y)|}{d(x, y)}$, denote the Lipschitz constant of f with respect to the metric d . Kantorovich metric is the IPM associated with the generating set: $\mathcal{W}_d \equiv \{f : \mathcal{X} \mapsto \mathbb{R} \mid \|f\|_d \leq 1\}$.

MMD: Let k be a characteristic kernel [Sriperumbudur et al., 2011] over the domain \mathcal{X} . Let $\|f\|_k$ denote the norm of f in the canonical RKHS, \mathcal{H}_k , corresponding to k . Maximum Mean Discrepancy (MMD) is the IPM associated with the generating set: $\mathcal{M}_k \equiv \{f \in \mathcal{H}_k \mid \|f\|_k \leq 1\}$.

Total Variation: This is the IPM associated with the generating set: $\mathcal{T} \equiv \{f : \mathcal{X} \mapsto \mathbb{R} \mid \|f\|_{\infty} \leq 1\}$, where $\|f\|_{\infty} \equiv \max_{x \in \mathcal{X}} |f(x)|$.

Dudley: This is the IPM associated with the generating set: $\mathcal{D}_c \equiv \{f : \mathcal{X} \mapsto \mathbb{R} \mid \|f\|_{\infty} + \|f\|_c \leq 1\}$, where c is a ground metric over \mathcal{X} .

Kolmogorov: Let $\mathcal{X} = \mathbb{R}^n$. Then, Kolmogorov metric is the IPM associated with the generating set: $\mathcal{K} \equiv \{1_{(-\infty, x]} \mid x \in \mathbb{R}^n\}$.

Like divergences, the IPMs can also be readily employed for comparing un-normalized measures. Some well-known advantages of IPMs over ϕ -divergences are:

- IPMs are well-defined and meaningful even for measures with disjoint support, whereas ϕ -divergences are infinite in such cases.
- Estimators of IPMs (with continuous measures, say) are (typically) well-behaved. Whereas in case of, say KL divergence, the rate of convergence can be too slow for some measures. In general, estimators of IPMs converge faster than those of divergences.
- IPMs like the Wasserstein/Dudley/MMD may provide more natural geometries than ϕ -divergences, whenever the cost/kernel is aligned with the ground metric (over \mathcal{X}). Whereas, divergences are typically agnostic to the ground geometry.

2.2 Optimal Transport

Given a cost function, $c : \mathcal{X} \times \mathcal{X} \mapsto \mathbb{R}$, and two probability measures $\mu \in \mathcal{R}_1(\mathcal{X}), \nu \in \mathcal{R}_1(\mathcal{X})$, the Kantorovich OT formulation is given by:

$$\begin{aligned} \min_{\pi \in \mathcal{R}_1(\mathcal{X} \times \mathcal{X})} \quad & \int_{\mathcal{X} \times \mathcal{X}} c \, d\pi \\ \text{s.t.} \quad & \pi_1 = \mu, \pi_2 = \nu. \end{aligned} \quad (2)$$

An optimal solution of (2) is called as a transport plan and has applications in domain adaptation [Courty et al., 2017] etc. Whenever the cost is a metric over \mathcal{X} (ground metric), the optimal objective defines another metric, known as the Wasserstein metric, over $\mathcal{R}_1(\mathcal{X})$. In particular, the optimal objective is the Wasserstein distance between μ, ν . This has many applications: as a loss function [Frogner et al., 2015], for measure interpolation [Gramfort et al., 2015], etc. In this case, the Kantorovich duality result shows that the Wasserstein metric is same as the Kantorovich metric with the same ground metric.

In cases where the given measures are un-normalized and may be of unequal masses, known as the unbalanced optimal transport (UOT) setting, or when the measures are noisy, one employs a regularized version:

$$\min_{\pi \in \mathcal{R}(\mathcal{X} \times \mathcal{X})} \int_{\mathcal{X} \times \mathcal{X}} c \, d\pi + \lambda_1 D_{\phi}(\pi_1, \mu) + \lambda_2 D_{\phi}(\pi_2, \nu), \quad (3)$$

where D_{ϕ} is the divergence generated by ϕ . For example, Liero et al. [2018] studies the metric properties of (3) in the special case of the KL-divergence based regularization:

$$K_c^{\lambda_1, \lambda_2}(\mu, \nu) \equiv \min_{\pi \in \mathcal{R}(\mathcal{X} \times \mathcal{X})} \int_{\mathcal{X} \times \mathcal{X}} c \, d\pi + \lambda_1 KL(\pi_1, \mu) + \lambda_2 KL(\pi_2, \nu), \quad (4)$$

3 Proposed IPM-regularized OT

Motivated by the attractive features of Integral Probability Metric (IPM) estimators over ϕ -divergence estimators [Sriperumbudur et al., 2009], we propose and study the following novel formulation for regularized OT:

$$\mathcal{U}_{\mathcal{G},c}^{\lambda_1,\lambda_2}(\mu,\nu) \equiv \min_{\pi \in \mathcal{R}(\mathcal{X} \times \mathcal{X})} \int_{\mathcal{X} \times \mathcal{X}} c \, d\pi + \lambda_1 \gamma_{\mathcal{G}}(\pi_1, \mu) + \lambda_2 \gamma_{\mathcal{G}}(\pi_2, \nu), \quad (5)$$

where $\gamma_{\mathcal{G}}$ is the IPM associated with the generating set \mathcal{G} , $\lambda_i \geq 0$ are regularization hyperparameters. We now study the dual and metric properties of (5). As mentioned earlier, such properties are well-understood for ϕ -divergence based regularizers. However, to the best of our knowledge, IPM regularizers have not been studied for OT problems.

3.1 Dual of the Proposed Formulation

We begin with a simple lemma and an associated assumption.

Assumption 1. *The generating set, \mathcal{G} , is absolutely convex, (pointwise) bounded, and closed subset of continuous functions over \mathcal{X} .*

Lemma 1. *Consider the IPM definition (1). Without loss of generality, Assumption 1 holds.*

It should be noted that under Assumption 1, $f \in \mathcal{G} \Rightarrow -f \in \mathcal{G}$, and hence $\gamma_{\mathcal{G}}(\mu, \nu) = \max_{f \in \mathcal{G}} \int_{\mathcal{X}} f \, d\mu - \int_{\mathcal{X}} f \, d\nu$. Additionally, we assume that the IPM $\gamma_{\mathcal{G}}$ is well-behaved as formalized below:

Assumption 2. $\lim_{n \rightarrow \infty} \gamma_{\mathcal{G}}(\mu_n, \nu_n) = \gamma_{\mathcal{G}}(\mu, \nu)$, for all weakly convergent sequences $\{\mu_n\} \rightarrow \mu$, $\{\nu_n\} \rightarrow \nu$.

Under these mild assumptions, it follows (from Theorem 4.3 in Muller [1997] and the Arzelà–Ascoli theorem) that \mathcal{G} is a compact set. We now present a key theorem regarding the dual of the proposed formulation (5).

Theorem 1. *Under Assumptions 1&2, an equivalent (Kantorovich-type) Fenchel dual of the proposed formulation (5) is:*

$$\mathcal{U}_{\mathcal{G},c}^{\lambda_1,\lambda_2}(\mu,\nu) = \max_{\substack{f \in \mathcal{G}(\lambda_1), g \in \mathcal{G}(\lambda_2) \\ \text{s.t.} \\ f(x) + g(y) \leq c(x,y) \, \forall x, y \in \mathcal{X}}} \int_{\mathcal{X}} f \, d\mu + \int_{\mathcal{X}} g \, d\nu, \quad (6)$$

where $\mathcal{G}(\lambda) \equiv \{\lambda f \mid f \in \mathcal{G}\}$.

The proof follows by writing the definition of the IPM and interchanging the min-max under the assumptions.

3.2 Metric Properties

Metric properties of the proposed formulation (5) follow from the corollary below:

Corollary 1. *In case the cost function c is a (ground) metric over \mathcal{X} , and $0 \leq \lambda \equiv \lambda_1 = \lambda_2$, then the dual formulation (6) further simplifies as:*

$$\mathcal{U}_{\mathcal{G},c}^{\lambda}(\mu,\nu) \equiv \mathcal{U}_{\mathcal{G},c}^{\lambda,\lambda}(\mu,\nu) = \max_{f \in \mathcal{G}(\lambda) \cap \mathcal{W}_c} \int_{\mathcal{X}} f \, d\mu - \int_{\mathcal{X}} f \, d\nu. \quad (7)$$

As discussed in Section 2.1, \mathcal{W}_c is the canonical generating set of the Kantorovich metric, which is the set of all 1-Lipschitz functions under the ground metric c . The corollary follows from standard results in c -conjugacy (c -transforms) and discussed in more detail in the supplementary material. From this dual, it is clear that \mathcal{U} lifts the ground metric to that over $\mathcal{M}(\mathcal{X})$:

Corollary 2. *Under Assumptions 1&2, and cost c being a metric, \mathcal{U} defines a family of metrics over $\mathcal{M}(\mathcal{X})$. By changing \mathcal{G} , $\lambda \geq 0$, and c , one can realize various metrics in this family. For a given \mathcal{G} , $\lambda \geq 0$, and c , $\mathcal{U}_{\mathcal{G},c}^{\lambda}$ is the IPM corresponding to the generating set $\mathcal{G}(\lambda) \cap \mathcal{W}_c$.*

In the special case where the regularizer is a Kantorovich metric based, i.e., $\mathcal{G} = \mathcal{W}_c$ and $\lambda \geq 1$, the proposed metric \mathcal{U} turns out to be a Kantorovich metric itself. Thus, in this case, the proposed formulation (5) generalizes the ‘‘primal/Wasserstein’’ definition to arbitrary measures, which exactly corresponds to the Kantorovich metric.

This observation motivates us to generalize our definition and define the following family of loss functions, analogous to the p -Wasserstein metrics:

$$\mathcal{U}_{\mathcal{G},c}^{\lambda_1,\lambda_2,p,q}(\mu,\nu)^p \equiv \min_{\pi \in \mathcal{R}(\mathcal{X} \times \mathcal{X})} \int_{\mathcal{X} \times \mathcal{X}} c^p \, d\pi + \lambda_1 \gamma_{\mathcal{G}}(\pi_1, \mu)^q + \lambda_2 \gamma_{\mathcal{G}}(\pi_2, \nu)^q. \quad (8)$$

Here, $p \geq 1, q \geq 1$ are user-provided hyperparameters.

A related problem of interest is the Barycenter problem: given measures s_1, \dots, s_k , with total masses $\sigma_1, \dots, \sigma_k$ respectively, and interpolation weights ρ_1, \dots, ρ_k , the Barycenter $s \in \mathcal{R}(X)$ is defined as the solution of the following problem:

$$\min_{s \in \mathcal{R}(X)} \sum_{i=1}^k \rho_i \mathcal{U}_{\mathcal{G},c}^{\lambda_1, \lambda_2, p, q}(s_i, s)^p \quad (9)$$

3.3 Algorithms

In general, (7) can be estimated and using techniques detailed in Sriperumbudur et al. [2012]. With the classical IPM-regularizers except MMD, this essentially amounts to solving a linear program. In case of MMD, an additional norm constraint appears (resulting in conic-quadratic problem).

Again, assuming the transport plan is supported only over the given samples, (8) can be estimated using projected gradient descent (pgd), or mirror-descent/Frank-Wolfe methods (if the transport plan is to be normalized). The gradient can be computed using the witness functions of the two IPM terms, which in turn can be estimated using techniques in Sriperumbudur et al. [2012], i.e., by solving a linear program (analytical form known in case of MMD).

Squared-MMD regularization. Estimation in case of squared-MMD regularizer, i.e., with \mathcal{G} is unit-ball in RKHS, and $q = 2$ in (8), is particularly simple. To this end, let $s_1 \equiv \mu$ and $s_2 \equiv \nu$ be the given measures with total masses σ_1 and σ_2 , respectively. Let m_i samples from s_i be given¹: $\mathcal{D}_i = \{x_{i1}, \dots, x_{im_i}\}$. Let us denote the Gram-matrix with \mathcal{D}_i under a given (characteristic) kernel as G_{ii} . Let \mathcal{C}_{12} be the $m_1 \times m_2$ cost matrix with entries as evaluations of c^p over $\mathcal{D}_1 \times \mathcal{D}_2$. As mentioned earlier, let us assume the transport plan is supported only at the samples²: let $\alpha_{ij} \equiv \pi(x_{1i}, x_{2j})$. Then, (8) simplifies as (10) below:

$$\min_{\alpha \geq 0 \in \mathbb{R}^{m_1 \times m_2}} \text{tr}(\alpha \mathcal{C}_{12}^\top) + \lambda_1 \|\alpha \mathbf{1} - \frac{\sigma_1}{m_1} \mathbf{1}\|_{G_{11}}^2 + \lambda_2 \|\alpha^\top \mathbf{1} - \frac{\sigma_2}{m_2} \mathbf{1}\|_{G_{22}}^2. \quad (10)$$

Here, $\|x\|_M^2 \equiv x^\top M x$. Employing pgd/mirror-descent for solving (10) is particularly simple as the gradient computation as well as line-search for step size are straight-forward.

The barycenter estimation problem (9) in this special case admits an elegant form. Let m_i samples from s_i be given: $\mathcal{D}_i = \{x_{i1}, \dots, x_{im_i}\}$. Let us denote the Gram-matrix with \mathcal{D}_i as G_i and that with $\cup_{i=1}^k \mathcal{D}_i$ as G . Let \mathcal{C}_i be the $m_i \times m$ matrix with entries as evaluations of cost function, c^p . Then, the proposed Barycenter formulation simplifies as:

$$\min_{\alpha_i \geq 0 \in \mathbb{R}^{m_i \times m} \forall i} \sum_{i=1}^k \rho_i \left\{ \text{tr}(\alpha_i \mathcal{C}_i^\top) + \lambda_1 \left\| \alpha_i \mathbf{1} - \frac{\sigma_i}{m_i} \mathbf{1} \right\|_{G_i}^2 + \lambda_2 \left\| \alpha_i^\top \mathbf{1} - \sum_{j=1}^k \rho_j \alpha_j^\top \mathbf{1} \right\|_G^2 \right\} \quad (11)$$

Problem (11) can be solved efficiently using the projected gradient-descent or the mirror-descent algorithm. Once (11) is solved, one can retrieve the Barycenter using the expression: $\sum_{j=1}^k \rho_j \alpha_j^\top \mathbf{1}$.

4 Experiments

In this section, we empirically evaluate the proposed MMD regularized (unbalanced) OT formulation (10) and compare it with the popular KL-divergence regularized (unbalanced) OT formulation (4). The two formulations are henceforth referred to as MMD-UOT and KL-UOT, respectively. We begin with a qualitatively comparing the transport plans obtained from the both the formulations on one dimensional Gaussian setting and then discuss results on single cell RNA sequencing and class-ratio estimation problems.

4.1 Transport plans with unbalanced Gaussian measures

Experimental setup: We take one-dimensional samples of size 100 ranging from 0 to 99 for both source and the target. The source measure is a Gaussian over the samples with mean as 20, standard deviation as 5 and total mass as 1. The target measure is a Gaussian over the samples with mean as 60, standard deviation as 10 and total mass as 5. Squared Euclidean distance is used to compute the cost matrix and Gaussian kernel was used as characteristic kernel. Unbalanced Sinkhorn algorithm is used from Python OT Flamary et al. [2021] to solve KL-UOT. The formulation given in Eq(8) is used for the proposed method with the IPM as MMD, p as 2 & q as 2.

¹Like in ML applications, we assume that the measures s_i themselves are not known. They are only known through samples.

²Alternatively, we can assume the support is $\mathcal{D}_1 \cup \mathcal{D}_2$ on both sides.

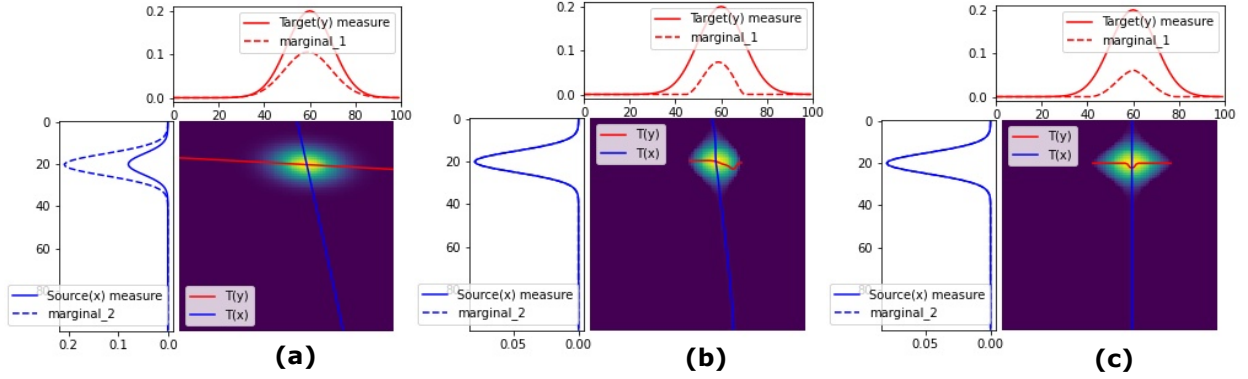

 Figure 1: Transport plans with $p = 2$ for (a) KL-UOT (b) Proposed(i), (c) Proposed(ii)

Table 1: Earth Mover Distance (EMD) on scRNA-seq experiments (lesser is better)

Method	t1	t2	t3
Avg	1.160	0.583	0.451
KL-UOT	1.075	0.613	0.455
Proposed	0.969	0.547	0.442

Evaluation & Results: Fig 4.1 shows transport maps, transport plans and the corresponding marginals obtained by the proposed algorithm and by KL-UOT. All transport matrices(plans) shown are normalized between 0 (blue) and 1 (yellow). Figure 4.1(b) and Figure 4.1(c) show the transport plan with the proposed formulation with different regularization parameters (λ_1 and λ_2). As discussed in Janati et al. [2020], the transport plan obtained with KL-UOT (with entropic regularization) turn out to be a Gaussian measure. The proposed UOT regularized with MMD squared shows diverse results depending on the hyper-parameters. Additionally, Proposed(ii) is a result where the support of our transport plan differs from the support of KL-UOT.

4.2 Single cell RNA sequencing

Single cell RNA sequencing technique (scRNA-seq) have received increased attention in developmental biology as it provides insights into cellular functionality by recording expression profiles of genes [Kolodziejczyk et al., 2015, Wagner et al., 2016]. One popular application of this technology is to understand how the expression profile of the cells change over stages [Schiebinger et al., 2019], e.g., from embryonic stem cells to specified lineages such as hematopoietic or neuronal. An expression profile is a mathematical expression of cells as vectors in gene expression space, where each dimension corresponds to gene. A population of cells is represented as a measure on the gene expression space and as they grow/divide/die, the measure evolves over time. Overall, scRNA-seq records such a measure (on the gene expression space) of a population of cells at a time stamp, but does so by destroying the cells [Schiebinger et al., 2019]. Thus, it is not possible to monitor how the cell population evolve continuously over time. In fact, only a few measurements at discrete timesteps are generally taken due to the cost involved.

Barycenter in the optimal transport framework offers a principled approach to estimate the trajectory of a measure at an intermediate timestep t ($t_i < t < t_j$) when we have measurements available only at t_i (source) and t_j (target) time steps.

Experimental setup: We perform experiments on Embryoid Body (EB) single cell dataset [Moon et al., 2019]. The dataset has samples available at five timesteps (t_j with $j = 0, \dots, 4$) which were collected during a 25-day period of development of human embryo. Following Tong et al. [2020], we project the data onto two-dimensional space and associate uniform measures to the source and the target samples given at different timesteps. We consider the samples at timestep t_i and t_{i+2} as the samples from the source and target measures where $0 \leq i \leq 2$ and aim at estimating the measure at t_i timestep as their barycenter with equal interpolation weights $\rho_1 = \rho_2 = 0.5$. The barycenter of the measures are computed using the proposed MMD-UOT (11) and the KL-UOT [Chizat et al., 2018, Liero et al., 2018]. For both proposed MMD-UOT and KL-UOT barycenter formulations, simplex constraint is used to cater to the case of uniform measures. The ground metric was taken as squared Euclidean distance and the Gaussian kernel was used

Table 2: Average absolute deviation (lesser is better) on class-ratio estimation experiments

Dataset	KL-UOT	Proposed
Australian	0.057	0.014
SAHeart	0.169	0.038
Ionosphere	0.191	0.288
Diabetes	0.193	0.190

as characteristic kernel for MMD. We also report results on the average barycenter, obtained by taking an empirical mean of the source and the target measures. The computed barycenter is evaluated against the measure corresponding to the ground truth samples available at that timestep. We compute the distance between two using the Earth Mover Distance(EMD).

Results: The results are reported in Table 1. We observe that the proposed method outperforms the baselines on all the three timesteps. It should also be noted that the performance of KL-UOT worse than the simple average baseline in two out of three timesteps.

4.3 Class ratio estimation

We next consider the class ratio estimation problem [Iyer et al., 2014]. Given a multi-class labeled training dataset $L = \{x_i, y_i\}_{i=1}^{m_1}$, the aim is to estimate the ratio of classes in an unlabeled test dataset $U = \{x_j\}_{j=m_1+1}^{m_2}$ (in the same input/output space). Here, $x \in \mathbb{R}^d$ and $y \in Y$, where $Y = \{1, \dots, c\}$ is the set of all labels. It should be noted that the distribution of classes in the labeled dataset may be different from the unlabeled dataset. Thus, while $P_L(y) \neq P_U(y)$, following existing works [Zhang et al., 2013, Iyer et al., 2014], we assume that $P(x|y)$ remains unchanged across datasets. Lets assume an unknown $\theta \in \Delta_c$, where $\Delta_c := \{z \in \mathbb{R}^c | z \geq \mathbf{0}; \sum_i z_i = 1\}$, is the class ratio in the test dataset, i.e, $P_U(y) = \theta$. Then, a distribution $Q(x) = \sum_{i=1}^c P_L(x|y = i)\theta_i$ should match the test distribution $P_U(x)$.

It should be noted that ϕ -divergence based loss function cannot be used to learn class distribution θ as the support of distributions $Q(x)$ and $P_U(x)$ are different. Existing works [Zhang et al., 2013, Iyer et al., 2014] employ IPM such as MMD to learn the distribution θ . In this work, we employ the proposed squared MMD regularized UOT formulation as follows:

$$\min_{\theta \in \Delta_c} \min_{\substack{\alpha \in \mathbb{R}^{m_1 \times m_2} \\ \alpha \geq \mathbf{0}, \mathbf{1}^\top \alpha \mathbf{1} = 1}} tr(\alpha C_{12}^\top) + \lambda_1 \|\alpha \mathbf{1} - z(\theta)\|_{G_{11}}^2 + \lambda_2 \|\alpha^\top \mathbf{1} - \frac{1}{m_2} \mathbf{1}\|_{G_{22}}^2, \quad (12)$$

where $z(\theta) \in \mathbb{R}^{m_1}$, $z_i(\theta) = \frac{\theta_{y_i}}{n_{y_i}}$, and n_j denotes the number of instances labeled j in L . Similarly, the KL-divergence regularized UOT formulation (4) for class-ratio estimation problem is as follows:

$$\min_{\theta \in \Delta_c} \min_{\substack{\alpha \in \mathbb{R}^{m_1 \times m_2} \\ \alpha \geq \mathbf{0}, \mathbf{1}^\top \alpha \mathbf{1} = 1}} tr(\alpha C_{12}^\top) + \lambda_1 KL(\alpha \mathbf{1}, z(\theta)) + \lambda_2 KL(\alpha^\top \mathbf{1}, \frac{1}{m_2} \mathbf{1}). \quad (13)$$

Experimental setup: We follow the experimental setup described in Iyer et al. [2014] and show results on four binary classification datasets from the UCI repository [Dua and Graff, 2017]. The fraction of positive class examples on the training set is fixed as 0.5. For each dataset, we create four test set with the fraction of positive class examples as [0.2, 0.4, 0.6, 0.8]. For every dataset, we report the average absolute deviation from this ground truth.

Evaluation & Results: The results are reported in Table 2. We observe that the proposed formulation is better than KL-UOT in three out of four datasets. This shows that the proposed IPM-regularization based OT is a viable alternative to ϕ -divergence based OT.

5 Remarks and Discussion

In this section we present some insightful remarks and discussions that are aligned with our work. We begin with a connection of regularization with robustness. While this discussion is relevant for both divergence and IPM based regularizers, we present the details only for the IPM case for the sake of simplicity.

5.1 Regularization and Robustness

One of the argued benefits of regularization is robustness to noisy/uncertain marginals. Contrary to the popular belief, in the discussion below, we show that such a regularization is beneficial when OT is used as a gain function rather than a loss function.

Let us assume that the marginals, $\hat{\mu}, \hat{\nu}$, are noisy: for e.g., they may be estimated from samples. We assume that the true marginals, μ, ν , lie within an appropriate ball around $\hat{\mu}, \hat{\nu}$. Here we make a fairly liberal assumption that $\gamma_{\mathcal{G}}(\mu, \hat{\mu}) \leq \epsilon, \epsilon > 0$.

Following the principle of robust optimization, we formulate the corresponding robust optimal transport problem as:

$$\begin{aligned} \min_{\mu \in \mathcal{R}_1(\mathcal{X}), \nu \in \mathcal{R}_1(\mathcal{X})} \quad & \mathbb{W}_c(\mu, \nu), \\ \text{s.t.} \quad & \gamma_{\mathcal{G}}(\mu, \hat{\mu}) \leq \epsilon, \gamma_{\mathcal{G}}(\nu, \hat{\nu}) \leq \epsilon, \end{aligned} \tag{14}$$

where $\mathbb{W}_c(\mu, \nu)$ is the Wasserstein metric induced by ground metric, c , if μ, ν are probability measures. Note that alternatively, we could have formulated robust OT as:

$$\begin{aligned} \max_{\mu \in \mathcal{R}_1(\mathcal{X}), \nu \in \mathcal{R}_1(\mathcal{X})} \quad & \mathbb{W}_c(\mu, \nu), \\ \text{s.t.} \quad & \gamma_{\mathcal{G}}(\mu, \hat{\mu}) \leq \epsilon, \gamma_{\mathcal{G}}(\nu, \hat{\nu}) \leq \epsilon, \end{aligned} \tag{15}$$

Either option is fine as long as it is used in an appropriate application. In particular, (15) is well-suited for applications where the robust OT is employed as a loss function (e.g., Frogner et al. [2015]). This is because for a minimization objective (over model parameters perhaps) indeed the worst-case setting is when the true marginals are located such that the Wasserstein distance is the maximum possible. Analogously, (14) is well-suited for applications where the robust OT is employed as a gain function (e.g., Flamary et al. [2018]).

The Tikhonov form of (14) is:

$$\min_{\mu \in \mathcal{R}_1(\mathcal{X}), \nu \in \mathcal{R}_1(\mathcal{X})} \quad \mathbb{W}_c(\mu, \nu) + \lambda \gamma_{\mathcal{G}}(\mu, \hat{\mu}) + \lambda \gamma_{\mathcal{G}}(\nu, \hat{\nu}), \tag{16}$$

where λ is an appropriate regularization parameter. Needless to say, as $\lambda \rightarrow \infty$ (i.e., $\epsilon \rightarrow 0$), and in case $\hat{\mu}, \hat{\nu}$ are probability measures, then (16) is same as standard Optimal Transport problem, leading to the Wasserstein metric. In this regard, we have the following result.

Lemma 2. *At optimality, (16) is equal to $\mathcal{U}_{\mathcal{G},c}^{\lambda}(\hat{\mu}, \hat{\nu})$.*

In other words, the proposed metrics (analogously the divergence regularized ones) can be interpreted as robust variants of classical Wasserstein metrics. More importantly, they are well-suited for applications where OT is to be employed as a gain rather than a loss function.

5.2 Flexible Parameterization

A key advantage of IPM based regularization over KL based regularization is flexibility in parameterization for estimation. For example, in the context of (10), we could have parametrized the plan using all examples, $\mathcal{D}_1 \cup \mathcal{D}_2$, on both sides, leading to:

$$\begin{aligned} \min_{\alpha \geq 0 \in \mathbb{R}^{m \times m}} \quad & \text{tr}(\alpha \mathcal{C}^{\top}) + \lambda_1 \left(\mathbf{1}^{\top} \alpha^{\top} G \alpha \mathbf{1} + \frac{\sigma_1^2}{m_1^2} \mathbf{1}^{\top} G_{11} \mathbf{1} - 2 \frac{\sigma_1}{m_1} \mathbf{1}^{\top} [G_{11} G_{12}] \alpha \mathbf{1} \right) \\ & + \lambda_2 \left(\mathbf{1}^{\top} \alpha G \alpha^{\top} \mathbf{1} + \frac{\sigma_2^2}{m_2^2} \mathbf{1}^{\top} G_{22} \mathbf{1} - 2 \frac{\sigma_2}{m_2} \mathbf{1}^{\top} [G_{21} G_{22}] \alpha^{\top} \mathbf{1} \right) \end{aligned} \tag{17}$$

However, parameterization in divergence based regularization is severely restricted because for example, the support of α on i^{th} side cannot be larger than that of \mathcal{D}_i etc. Figure 1 also confirms that meaningful solutions are obtained with IPM regularization in cases of difference in support. This feature might be useful in cases where support constraints for the transport plan exist [Korman and McCann, 2012].

6 Conclusion

In the context of OT, IPM based regularization is not well-understood. This work studies some prima facie characteristics of this regularization. Given the advantages of IPMs over divergences, this indeed seems to be a line of study with immense potential in ML applications.

We show that some IPM regularization of lifts ground metrics to those over (arbitrary) measures. Moreover, the lifted metric turns out to be another IPM.

The special case of squared-MMD (among IPM regularizers) seemingly is analogous to KL-divergence (among ϕ -divergences), in the sense that it leads to some simplifications. In particular, the corresponding OT and barycenter problems can be solved efficiently. Also, it seems to outperform KL-regularization in Biological interpolation applications.

Broader Impact

This work complements the ongoing research towards a better understanding of optimal transport problems. Our contributions are mainly theoretical, with novel regularized optimal transport formulations, with some empirical results on single cell RNA sequencing and class-ratio estimation problems. Overall, we aim to provide better solutions to such problems and do not foresee any negative societal consequence.

References

- Rohit Agrawal and Thibaut Horel. Optimal bounds between f-divergences and integral probability metrics. In *Proceedings of the 37th International Conference on Machine Learning*, 2020.
- L. Chizat, G. Peyre, B. Schmitzer, and F.-X. Vialard. Unbalanced optimal transport: Dynamic and kantorovich formulations. *Journal of Functional Analysis*, 274(11):3090–3123, 2018.
- Lenaïc Chizat. Unbalanced optimal transport : Models, numerical methods, applications. Technical report, 2017.
- Nicolas Courty, Rémi Flamary, Amaury Habrard, and Alain Rakotomamonjy. Joint distribution optimal transportation for domain adaptation. In *Advances in Neural Information Processing Systems*, volume 30, pages 3730–3739, 2017.
- Marco Cuturi. Sinkhorn distances: Lightspeed computation of optimal transport. In *Proceedings of the 26th International Conference on Neural Information Processing Systems - Volume 2*, page 2292–2300, 2013.
- Dheeru Dua and Casey Graff. UCI machine learning repository, 2017. URL <http://archive.ics.uci.edu/ml>.
- Jean Feydy, Thibault Séjourné, François-Xavier Vialard, Shun ichi Amari, Alain Trounev, and Gabriel Peyré. Interpolating between optimal transport and mmd using sinkhorn divergences. In *International Conference on Artificial Intelligence and Statistics*, 2018.
- Rémi Flamary, Marco Cuturi, Nicolas Courty, and Alain Rakotomamonjy. Wasserstein discriminant analysis. *Machine Learning*, 107(12):1923–1945, 2018.
- Rémi Flamary, Nicolas Courty, Alexandre Gramfort, Mokhtar Z. Alaya, Aurélie Boisbunon, Stanislas Chambon, Laetitia Chapel, Adrien Corenflos, Kilian Fatras, Nemo Fournier, Léo Gautheron, Nathalie T.H. Gayraud, Hicham Janati, Alain Rakotomamonjy, Ievgen Redko, Antoine Rolet, Antony Schutz, Vivien Seguy, Danica J. Sutherland, Romain Tavenard, Alexander Tong, and Titouan Vayer. Pot: Python optimal transport. *Journal of Machine Learning Research*, 22(78):1–8, 2021. URL <http://jmlr.org/papers/v22/20-451.html>.
- Charlie Frogner, Chiyuan Zhang, Hossein Mobahi, Mauricio Araya-Polo, and Tomaso Poggio. Learning with a wasserstein loss. In *Proceedings of the 28th International Conference on Neural Information Processing Systems - Volume 2*, pages 2053–2061, 2015.
- Aude Genevay, Lénaïc Chizat, Francis Bach, Marco Cuturi, and Gabriel Peyré. Sample complexity of sinkhorn divergences. In *The 22nd International Conference on Artificial Intelligence and Statistics, AISTATS 2019, 16-18 April 2019, Naha, Okinawa, Japan*, pages 1574–1583, 2019.
- Alexandre Gramfort, Gabriel Peyré, and Marco Cuturi. Fast optimal transport averaging of neuroimaging data. In *Proceedings of 24th International Conference on Information Processing in Medical Imaging*, 2015.
- Arun Iyer, Saketha Nath, and Sunita Sarawagi. Maximum mean discrepancy for class ratio estimation. In *ICML*, 2014.
- Hicham Janati, Boris Muzellec, Gabriel Peyré, and Marco Cuturi. Entropic optimal transport between unbalanced gaussian measures has a closed form. In *Advances in Neural Information Processing Systems*, 2020.
- Aleksandra. A. Kolodziejczyk, Jong Kyoung Kim, Valentine Svensson, John. C. Marioni, and Sarah. A. Teichmann. The technology and biology of single-cell rna sequencing. *Molecular Cell*, 58(4):610–620, 2015.
- Jonathan Korman and R. McCann. Optimal transportation with capacity constraints. *Transactions of the American Mathematical Society*, 367:1501–1521, 2012.
- Matthias Liero, Alexander Mielke, and Giuseppe Savaré. Optimal entropy-transport problems and a new hellinger–kantorovich distance between positive measures. *Inventiones mathematicae*, 211(3):969–1117, 2018.

- Gonzalo Mena and Jonathan Niles-Weed. Statistical bounds for entropic optimal transport: sample complexity and the central limit theorem. In H. Wallach, H. Larochelle, A. Beygelzimer, F. d'Alché-Buc, E. Fox, and R. Garnett, editors, *Advances in Neural Information Processing Systems*, volume 32. Curran Associates, Inc., 2019. URL <https://proceedings.neurips.cc/paper/2019/file/5acdc9ca5d99ae66afdf1ee0e3b26b-Paper.pdf>.
- Kevin R. Moon, David van Dijk, Zheng Wang, Scott Gigante, Daniel B. Burkhardt, William S. Chen, Kristina Yim, Antonia van den Elzen, Matthew J. Hirn, Ronald R. Coifman, Natalia B. Ivanova, Guy Wolf, and Smita Krishnaswamy. Visualizing structure and transitions for biological data exploration. *Nature Biotechnology*, 37(12):1482–1492, 2019.
- Alfred Muller. Integral probability metrics and their generating classes of functions. *Advances in Applied Probability*, 29:429–443, 1997.
- Jagarlapudi Saketha Nath and Pratik Kumar Jawanpuria. Statistical optimal transport posed as learning kernel embedding. In *Advances in Neural Information Processing Systems*, 2020.
- Gabriel Peyré and Marco Cuturi. Computational optimal transport. *Foundations and Trends® in Machine Learning*, 11(5-6):355–607, 2019.
- Geoffrey Schiebinger, Jian Shu, Marcin Tabaka, Brian Cleary, Vidya Subramanian, Aryeh Solomon, Joshua Gould, Siyan Liu, Stacie Lin, Peter Berube, Lia Lee, Jenny Chen, Justin Brumbaugh, Philippe Rigollet, Konrad Hochedlinger, Rudolf Jaenisch, Aviv Regev, and Eric S. Lander. Optimal-transport analysis of single-cell gene expression identifies developmental trajectories in reprogramming. *Cell*, 176(4):928–943.e22, 2019.
- Vivien. Seguy, Bharath B. Damodaran, Remi Flamary, Nicolas Courty, Antoine Rolet, and Mathieu Blondel. Large-scale optimal transport and mapping estimation. In *International Conference on Learning Representations (ICLR)*, 2018.
- B. Sriperumbudur, K. Fukumizu, A. Gretton, B. Schölkopf, and G. Lanckriet. On the empirical estimation of integral probability metrics. *Electronic Journal of Statistics*, 6:1550–1599, 2012.
- Bharath K. Sriperumbudur, Kenji Fukumizu, Arthur Gretton, Bernhard Schölkopf, and Gert R. G. Lanckriet. On integral probability metrics, phi-divergences and binary classification. *arXiv preprint arXiv:0901.2698*, 2009.
- Bharath K. Sriperumbudur, Kenji Fukumizu, and Gert R. G. Lanckriet. Universality, characteristic kernels and RKHS embedding of measures. *Journal of Machine Learning Research*, 12:2389–2410, 2011.
- Alexander Tong, Jessie Huang, Guy Wolf, David Van Dijk, and Smita Krishnaswamy. TrajectoryNet: A dynamic optimal transport network for modeling cellular dynamics. In Hal Daumé III and Aarti Singh, editors, *Proceedings of the 37th International Conference on Machine Learning*, volume 119 of *Proceedings of Machine Learning Research*, pages 9526–9536. PMLR, 13–18 Jul 2020. URL <http://proceedings.mlr.press/v119/tong20a.html>.
- A. Wagner, A. Regev, and N. Yosef. Revealing the vectors of cellular identity with single-cell genomics. *Nature Biotechnology*, 34:1145–1160, 2016.
- K. Zhang, B. Scholkopf, K. Muandet, and Z. Wang. Domain adaptation under target and conditional shift. In *ICML*, 2013.

A Appendix: Proof of Lemma 1

Proof. Let $O[f] \equiv |\int_{\mathcal{X}} f d\mu - \int_{\mathcal{X}} f d\nu|$. Now, by triangle inequality, $O[\alpha f + \beta g] \leq |\alpha|O[f] + |\beta|O[g]$. Also, whenever $|\alpha| + |\beta| \leq 1$, we have that $|\alpha|O[f] + |\beta|O[g] \leq \max(O[f], O[g])$. Hence, $\max_{f \in \text{aconv}(\mathcal{G})} O[f] = \max_{f \in \mathcal{G}} O[f]$, where $\text{aconv}(S)$ is the absolute convex hull of S . Therefore, there is indeed no loss of generality by assuming \mathcal{G} is absolutely convex.

Let us now assume that \mathcal{G} is not point-wise bounded, then there exists some $x_0 \in \mathcal{X}$ such that $\max_{f \in \mathcal{G}} f(x_0) = \infty$. Consider for example, that μ, ν are equal except that at x_0 , where $\mu(x_0) = 1, \nu(x_0) = 0$. Then, $O[f] = f(x_0)$ and hence, $\gamma_{\mathcal{G}}(\mu, \nu) = \infty$, which is impossible for a metric. Hence \mathcal{G} must be point-wise bounded.

Note that $O[f]$ is a continuous function, as it is absolute value of a linear function. Hence from standard results in optimization, we have $\max_{f \in \mathcal{G}} O[f] = \max_{f \in \text{cl}(\mathcal{G})} O[f]$, where $\text{cl}(S)$ is the closure of the set S . Therefore, indeed there is no loss of generality by assuming that \mathcal{G} is closed.

Lastly, since the set of all continuous functions is dense in the set of all measurable functions, considering subsets of continuous functions is enough. \square

B Appendix: Derivation of Dual

We begin by re-writing IPMs using their definitions in (5):

$$\begin{aligned}
 \mathcal{U}_{\mathcal{G},c}^{\lambda_1,\lambda_2}(\mu,\nu) &\equiv \min_{\pi \in \mathcal{R}(\mathcal{X} \times \mathcal{X})} \int_{\mathcal{X} \times \mathcal{X}} c d\pi + \lambda_1 \left(\max_{f \in \mathcal{G}} \int_{\mathcal{X}} f d\mu - \int_{\mathcal{X}} f d\pi_1 \right) + \lambda_2 \left(\max_{g \in \mathcal{G}} \int_{\mathcal{X}} g d\nu - \int_{\mathcal{X}} g d\pi_2 \right), \\
 &= \min_{\pi \in \mathcal{R}(\mathcal{X} \times \mathcal{X})} \int_{\mathcal{X} \times \mathcal{X}} c d\pi + \left(\max_{f \in \mathcal{G}(\lambda_1)} \int_{\mathcal{X}} f d\mu - \int_{\mathcal{X}} f d\pi_1 \right) + \left(\max_{g \in \mathcal{G}(\lambda_2)} \int_{\mathcal{X}} g d\nu - \int_{\mathcal{X}} g d\pi_2 \right), \\
 &= \max_{f \in \mathcal{G}(\lambda_1), g \in \mathcal{G}(\lambda_2)} \int_{\mathcal{X}} f d\mu + \int_{\mathcal{X}} g d\nu + \min_{\pi \in \mathcal{R}(\mathcal{X} \times \mathcal{X})} \int_{\mathcal{X} \times \mathcal{X}} c d\pi - \int_{\mathcal{X}} f d\pi_1 - \int_{\mathcal{X}} g d\pi_2, \\
 &= \max_{f \in \mathcal{G}(\lambda_1), g \in \mathcal{G}(\lambda_2)} \int_{\mathcal{X}} f d\mu + \int_{\mathcal{X}} g d\nu + \min_{\pi \in \mathcal{R}(\mathcal{X} \times \mathcal{X})} \int_{\mathcal{X} \times \mathcal{X}} c - \bar{f} - \bar{g} d\pi, \\
 &= \max_{f \in \mathcal{G}(\lambda_1), g \in \mathcal{G}(\lambda_2)} \int_{\mathcal{X}} f d\mu + \int_{\mathcal{X}} g d\nu + \begin{cases} 0 & \text{if } f(x) + g(y) \leq c(x, y) \forall x, y \in \mathcal{X}, \\ -\infty & \text{otherwise} \end{cases} \\
 &= \max_{f \in \mathcal{G}(\lambda_1), g \in \mathcal{G}(\lambda_2)} \int_{\mathcal{X}} f d\mu + \int_{\mathcal{X}} g d\nu, \\
 &\quad \text{s.t. } f(x) + g(y) \leq c(x, y) \forall x, y \in \mathcal{X}.
 \end{aligned} \tag{18}$$

Here, $\bar{f}(x, y) \equiv f(x)$, $\bar{g}(x, y) \equiv g(y)$. The min-max interchange in the third equation is due to Sion's minmax theorem and \mathcal{G} being convex compact.

C Appendix: Simplification of Dual

Constraints in dual, (6), are equivalent to: $g(y) \leq \min_{x \in \mathcal{X}} c(x, y) - f(x) \forall y \in \mathcal{X}$. The RHS is nothing but the c -conjugate (c -transform) of f . From proposition 6 in Peyré and Cuturi [2019], whenever c is a metric, say $c = d$, we have: $\min_{x \in \mathcal{X}} d(x, y) - f(x) = \begin{cases} -f(y) & \text{if } f \in \mathcal{W}_d, \\ -\infty & \text{otherwise.} \end{cases}$ Thus the constraints are equivalent to: $g(y) \leq -f(y) \forall y \in \mathcal{X}, f \in \mathcal{W}_d$. By symmetry, we also obtain that $f(y) \leq -g(y) \forall y \in \mathcal{X}, g \in \mathcal{W}_d$. Now, since the dual, (6), seeks to maximize the objective with respect to g , and monotonically increases with values of g ; at optimality we have that $g(y) = -f(y) \forall y \in \mathcal{X}$. Note that this equality is possible to achieve as both $g, f \in \mathcal{G}(\lambda) \cap \mathcal{W}_d$. Eliminating g , one obtains (7).

D Appendix: Barycenter with Squared-MMD regularizer

We begin with deriving (10). The feasibility set and the cost term in the objective are straight-forward. The MMD term $MMD(\pi_1, \mu)^2 = \|\sum_{i=1}^{m_1} \sum_{j=1}^{m_2} \alpha_{ij} \phi(x_i) - \frac{\sigma_1}{m_1} \sum_{i=1}^{m_1} \phi(x_i)\|^2$, where ϕ is the canonical feature map of the kernel.

Table 3: Absolute Deviation(lesser is better) averaged across all seeds and all class ratios

Dataset	KL-UOT	Proposed	Proposed-Flexible
Australian	0.170±0.119	0.143±0.115	0.195±0.171
SAHeart	0.179±0.089	0.223±0.145	0.122±0.078
Ionosphere	0.193±0.136	0.126±0.126	0.154±0.086
Diabetes	0.134±0.09	0.107±0.110	0.174±0.098

With the given notation, this is same as $\|\alpha \mathbf{1} - \frac{\sigma_1}{m_1} \mathbf{1}\|_{G_{11}}^2$. Similarly the next objective term follows. This leads to the simplification (10).

Coming to (11), again the feasibility set, the cost (first) term and matching marginals (second) term are straight-forward. The third term comes from the following simplification: $\min_{s \in \mathcal{R}(\mathcal{X})} \sum_{i=1}^k \rho_i MMD(\pi_{i2}, s)^2 = \min_{\beta \geq 0 \in \mathbb{R}^m} \sum_{i=1}^k \rho_i \left\| \sum_{p=1}^m \sum_{q=1}^{m_p} \alpha_{iqp} \phi(z_p) - \sum_{p=1}^m \beta_p \phi(z_p) \right\|^2 = \min_{\beta \geq 0 \in \mathbb{R}^m} \sum_{i=1}^k \rho_i \left\| \alpha_i^\top \mathbf{1} - \beta \right\|_G^2 = \sum_{i=1}^k \rho_i \left\| \alpha_i^\top \mathbf{1} - \sum_{j=1}^k \rho_j \alpha_j^\top \mathbf{1} \right\|_G^2$. Here, β provides the parameterization for the barycenter. The advantage with squared-MMD regularizer is that we can conveniently eliminate β .

E Appendix: Connection to Robustness

The result follows by writing the definition of \mathbb{W}_c and then eliminating μ, ν using the two equations.

F Experiments

F.1 Transport Plans with unbalanced Gaussian measures

We obtain transport plans with the proposed formulation given in equation 10. We use Projected Gradient Descent with step sizes tuned according to the Armijo rule. In Figure 1 of the main paper, the results with KL-UOT were obtained with entropic regularization as 10^{-1} and KL regularizations as 1. For Proposed(i), σ was 1 and λ 's as (501, 0.7158). For Proposed(ii), σ was chosen as 0.25 and λ 's as (10^{10} , 10^7). For a sample x , the Barycentric projection based optimal transport map T is estimated as $T(x) \equiv \operatorname{argmin}_{y \in \mathcal{Y}} \mathbb{E}[c(y, Y)|x]$ where the cost metric c was squared euclidean in our experiments.

F.2 Single cell RNA sequencing

Embryoid Body dataset comprises of data at 5 timesteps with sample sizes as 2381, 4163, 3278, 3665 and 3332 respectively. Mirror Descent was used to solve the barycenter formulations for the proposed method as well as for KL-UOT, with step size as the inverse of infinity norm of the gradient. KL regularization coefficients and λ 's for the proposed method were chosen from the set $\{10^5, 10^6, 10^7, 10^8\}$. We chose σ for the Gaussian kernel from the set $\{10^{-7}, 10^{-6}, 10^{-5}\}$. Entropic regularization coefficient as 10^{-6} and KL regularization coefficients as 10^6 gave the best results for KL-UOT. For the proposed method, sigma as 10^{-6} gave the best results with λ 's at timesteps t_2 and t_3 as 10^4 and λ at timestep t_1 as 10^3 .

F.3 Class ratio estimation

We experimented on four UCI datasets- Australian, Ionosphere, SA-Heart and Diabetes. Based on an initial random seed, we divided the data into a training set and a test set. The (training set size, test set size) for Australian, Ionosphere, SA-Heart and Diabetes datasets were (454, 100), (172, 50), (192, 80) and (376, 100) respectively. Hyper-parameters were tuned on 30 validation sets that were randomly sampled from the training set. The ratio of classes in the training sets was kept as 0.5. We report the results on the test set with the best hyper-parameter after repeating the experiment with 4 initial random seeds. The KL regularization coefficient for KL-UOT and λ 's for the proposed method were chosen from $\{10^{-2}, 10^{-1}, 1, 10^1, 10^2\}$. Entropic regularization coefficient for KL-UOT was fixed as 10^{-6} . For the two Gaussian Gram matrices in the proposed formulation, we chose σ_1 from $\{10^{+1}, 10^0, 10^{-1}, 10^{-2}, 10^{-3}\}$ and σ_2 from $\{10^{-1}, 10^{-2}, 10^{-3}, 10^{-4}\}$.

Table 4: Absolute Deviation(lesser is better) averaged across all seeds for Ionosphere dataset

θ_0^*	KL-UOT	Proposed	Proposed-Flexible
0.2	0.387±0.009	0.113±0.078	0.143±0.148
0.4	0.199±0.013	0.173±0.147	0.134±0.066
0.6	0.018±0.004	0.079±0.111	0.174±0.020
0.8	0.169±0.005	0.136±0.182	0.162±0.096

Table 5: Absolute Deviation(lesser is better) averaged across all seeds for SAHeart dataset

θ_0^*	KL-UOT	Proposed	Proposed-Flexible
0.2	0.252±0.091	0.141±0.202	0.164±0.106
0.4	0.141±0.081	0.186±0.144	0.100±0.062
0.6	0.131±0.064	0.250±0.072	0.102±0.073
0.8	0.182±0.093	0.316±0.124	0.123±0.081

Table 6: Absolute Deviation(lesser is better) averaged across all seeds for Diabetes dataset

θ_0^*	KL-UOT	Proposed	Proposed-Flexible
0.2	0.205±0.066	0.079±0.073	0.228±0.130
0.4	0.104±0.077	0.092±0.095	0.182±0.118
0.6	0.094±0.087	0.091±0.103	0.180±0.034
0.8	0.135±0.114	0.166±0.170	0.104±0.071

Table 7: Absolute Deviation(lesser is better) averaged across all seeds for Australian dataset

θ_0^*	KL-UOT	Proposed	Proposed-Flexible
0.2	0.321±0.053	0.204±0.201	0.245±0.261
0.4	0.131±0.063	0.17±0.115	0.252±0.196
0.6	0.024±0.01	0.094±0.034	0.135±0.134
0.8	0.205±0.028	0.104±0.008	0.148±0.081

F.3.1 Flexible Parameterization

In order to test the efficacy of flexible parameterization of the proposed method(section 5.2), we repeat the class ratio experiment with the proposed formulation parametrized as follows:

$$\min_{\theta \in \Delta_c} \min_{\substack{\alpha \in \mathbb{R}^{m \times m} \\ \alpha \geq \mathbf{0}, \mathbf{1}^\top \alpha \mathbf{1} = 1}} \text{tr}(\alpha \mathcal{C}^\top) + \lambda_1 \left(\mathbf{1}^\top \alpha^\top G \alpha \mathbf{1} + z(\theta)^\top G_{11} z(\theta) - 2z(\theta)^\top [G_{11} G_{12}] \alpha \mathbf{1} \right) + \lambda_2 \left(\mathbf{1}^\top \alpha G \alpha^\top \mathbf{1} + \frac{1}{m_2} \mathbf{1}^\top G_{22} \mathbf{1} - 2 \frac{1}{m_2} \mathbf{1}^\top [G_{21} G_{22}] \alpha^\top \mathbf{1} \right) \quad (19)$$

The validation procedure remains the same as mentioned in section F.3. We chose λ 's from the set $\{10^{-2}, 10^{-1}, 10^0, 10^{+1}, 10^{+2}\}$ and σ from $\{10^2, 10^1, 10^0, 10^{-1}, 10^{-2}, 10^{-3}, 10^{-4}\}$. In the subsequent discussion, we refer this formulation as 'Proposed-Flexible'.

Our metric for evaluation is the absolute deviation averaged over all class ratios and all seeds. The proposed method was able to outperform KL-UOT on Australian, Ionosphere and Diabetes. Proposed-Flexible gave the best results on SA-Heart dataset. We additionally present the absolute deviation averaged across all seeds with varying true fractions θ_0^* for Ionosphere(table 4), Diabetes(table 6), Australian(table 7) and SA-Heart(table 5).